THE ROLE OF SOLVENT QUALITY AND OF COMPETITIVE ADSORPTION ON THE EFFICIENCY OF SUPERPLASTICIZERS IN ALKALI-ACTIVATED SLAG PASTES

C. Paillard[a,b], M. Aparicio Cordoba[a], N. Sanson[a], J.-B. d'Espinose de Lacaillerie[a],*

G. Ducouret[a], P. Boustingorry[b], M. Jachiet[b], C. Giraudeau[b] and V. Kocaba[b]

[a] Soft Matter Science and Engineering Laboratory (SIMM), UMR CNRS 7615, ESPCI Paris, Université PSL, Sorbonne Université, Paris, France

[b] CHRYSO SAINT-GOBAIN France, Sermaises-du-Loiret, France

ABSTRACT

The loss of dispersing ability by polycarboxylates ether superplasticizers in alkali-activated slag cements has been widely reported. However, no clear-cut explanation of this phenomenon can be found to date. Therefore, the behaviour of poly(methacrylate-g-poly(ethylene glycol)) superplasticizers in NaOH or Na_2CO_3 -activated slag pastes was investigated. The observed loss of efficiency of the polymer was not due to a specific property of the slag particles, nor to structural degradation of the polymer in the alkaline solutions. Actually, the ionic strength of the activating solution decreased the solvent quality and changed the polymer conformation, leading to a deterioration of the steric repulsion brought by the side-chains. Moreover, in the Na_2CO_3 -activated systems, the adsorption behaviour of the polymers was also significantly altered. Here, this was not caused by a low calcium concentration or by a preferential adsorption of the superplasticizer on calcite crystallites. The most plausible explanation was a competitive adsorption with CO_3^{2-} ions.

Keywords: cement, rheology, polymer, alkali activation, admixtures, solubility, PCE, MPEG

Corresponding author: jean-baptiste.despinose@espci.fr

1. INTRODUCTION

Alkali-activated slag, consisting of ground-granulated blast furnace slag and an alkaline activator, is a novel low carbon cementitious material receiving increased attention worldwide. This is mainly due to its reduced environmental impact compared to ordinary Portland cement (OPC) while having similar performances [1–4] .

Still, one major impediment remains regarding its use at a large scale: to cast and pump concrete or mortars properly, a high and time-controlled fluidity is needed. This property is usually obtained by adding superplasticizers to the mix, polymers which adsorb on the surface of cement grains and keep them from flocculating. One of the most widely used families of superplasticizers is made of comb-shaped polymers based on the polycarboxylate ether (PCE) chemical structure [5]. These superplasticizers consist in a – usually anionic – charged backbone which adsorbs on the anionic charged sites of the cement particles, thanks to a surface charge inversion by the calcium cations present in the interstitial solution. Grafted side-chains of polyethylene glycol (PEG) extend in the interstitial solution, inducing a steric repulsion which keeps the particles from flocculating [6–9].

Yet, many studies show that the traditional superplasticizers used in OPC have little or no dispersing efficiency in alkali-activated slag cements [10–12]. Different explanations have been suggested in the literature. They are schematically represented in Figure 1. A first possibility is the degradation of the polymer structure by the alkaline environments of the activating solutions [12,13]. The steric repulsion could also be impacted by a lack of solubility of the superplasticizers as proposed in the study of Conte and Plank [14]. Another explanation could be a lack of adsorption of the polymers on the slag's surface. This could be due either to a lower Ca^{2+} concentration in the interstitial solution, to a difference of surface chemistry between slag and clinker's particles [15,16], to competitive adsorptions between the superplasticizers and other anions in solution [17], or to a different affinity of the polymer between the slag grains

and the hydrates formed very early [18]. However, no conclusive explanation has so far transpired, and no satisfactory solution has been found to address the challenge of the fluidity control of alkali-activated cements.

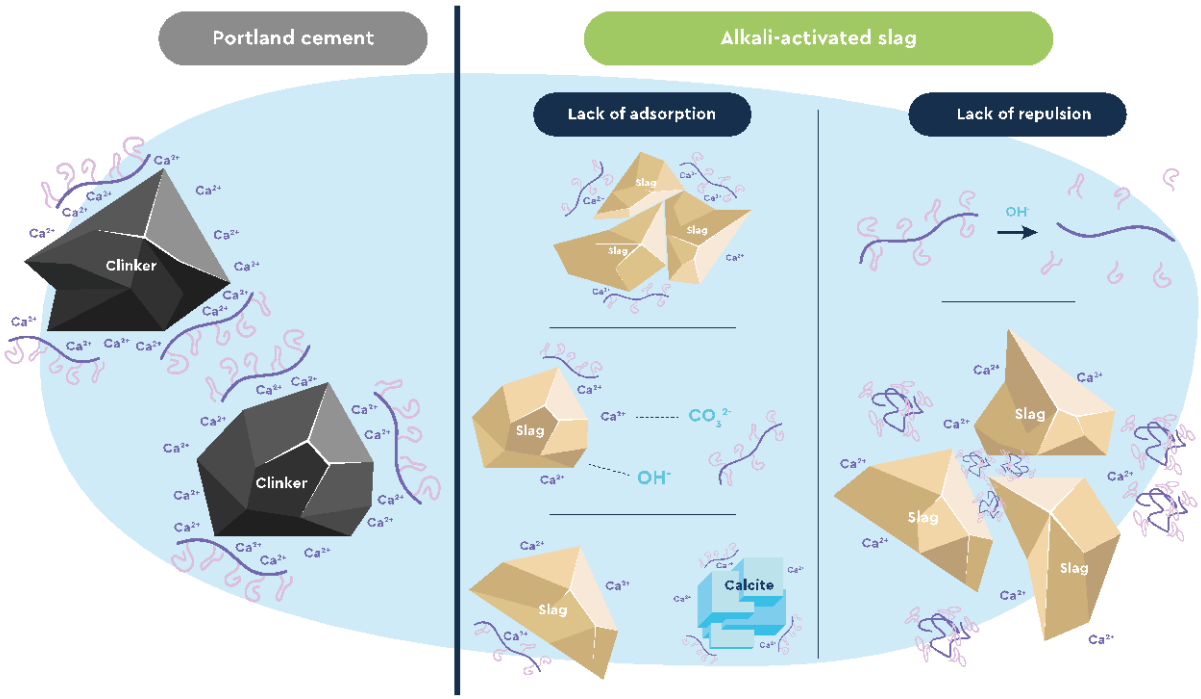

Figure 1: Schematic representation of the molecular origin of fluidification, or lack thereof, of clinker or activated slag pastes by PCEs. PCE adsorbs on clinker via charge inversion due to Ca^{2+}, and the swollen PEO side-chains prevents particle aggregation (left). This effect is lost in activated slag pastes. This could be explained by poor PCE adsorption due to an insufficient amount of Ca^{2+} (middle-top), to competitive adsorption between PCE and anions of the activating solutions (middle-centre), or to preferential adsorption of the PCE on precipitated very early reaction products such as calcium carbonates (middle-bottom). This could also be due to hydrolysis of the polymer (right- top) or to a collapse of the PEO side-chains (right-bottom) in the activating solution.

In this context, the aim of this study is to improve our understanding of the factors hindering the dispersing properties of polycarboxylates-based superplasticizers (PCE), a member of the poly(methacrylate-g-poly(ethylene glycol)) family also called MPEG, in slag cements activated

with NaOH or Na_2CO_3. For this purpose, the dispersing ability of the polymers was evaluated by rheological studies, and their chemical stability in the activating solutions was assessed by size exclusion chromatography. Moreover, adsorption measurements using the depletion method were used to investigate the affinity of the superplasticizer to the slag surface and determine if a competitive adsorption with the activator anions took place. These measurements were coupled to a study of the superplasticizer solubility and conformation using cloud point measurements and capillary viscometry. Finally, the interstitial concentration of calcium was measured by Inductively Coupled Plasma – Optical Emission Spectrometry (ICP-OES) and a possible competitive adsorption between slag and calcite was investigated.

2. MATERIALS AND METHODS

2.1. Materials

A ground granulated blast-furnace slag supplied by CHRYSO SAINT-GOBAIN France was used in this study. Its chemical composition, determined by X-ray fluorescence (XRF) by an external contractor (Université Paris Cité, France), is summarised in Table 1.

Table 1 : The chemical composition of the slag determined by XRF (wt %). LoI.: Loss on ignition measured at 1000 °C.

	SiO_2	CaO	Al_2O_3	Fe_2O_3	MgO	Na_2O	K_2O	TiO_2	MnO	LoI.
Slag	37.33	40.88	9.76	0.31	6.35	0.30	0.40	0.56	0.18	3.95

A specific surface area of 0.85 ± 0.02 m^2/g was measured by krypton adsorption following the BET method (see below). Figure 2a presents the particle size distribution of the slag dispersed in isopropanol and measured by laser light diffraction (Mastersizer, Malvern Panalytical), courtesy of Dr. Y. Keskin (Navier laboratory, Marne la Vallée, France), with a D_{v50} value of 9.15 µm. The particles have irregular shapes with sharp edges, as shown on the SEM image

(Figure 2b). The image was taken on a JEOL 6300F field emission electron microscope, at 10 kV, in high-vacuum mode.

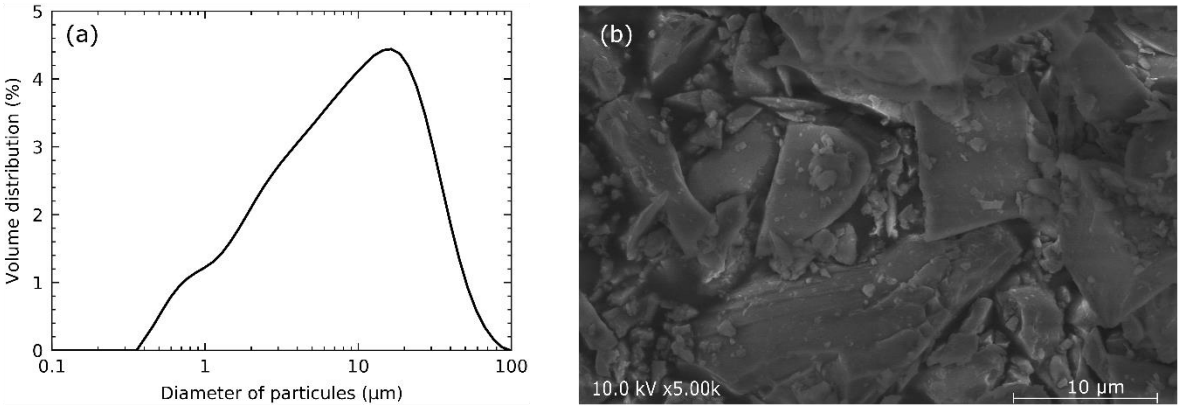

Figure 2: (a) Particle size distribution of the blast furnace slag. (b) SEM image of the blast furnace slag particles.

In some samples, the slag was replaced by a calcite powder from Sigma-Aldrich with a specific surface area of 0.58 ± 0.06 m^2/g, or one supplied by CHRYSO SAINT-GOBAIN France with a surface area of 2.1 ± 0.3 m^2/g.

Sodium hydroxide (NaOH) pellets EMPLURA® or sodium carbonate (Na_2CO_3) powder >99.5% from Sigma-Aldrich were used for the preparation of the activating solutions. Each were dissolved in ultrapure water (conductivity of 18.2 mΩ/cm) in the appropriate amounts in order to obtain an alkaline solution with the target activator's concentration. With some exceptions (as specified), the activating solutions had a composition corresponding to a paste formulation of 4.0 % Na_2O by weight of slag and a water/slag (w/s) weight ratio of 0.4. This composition allowed having a reasonable setting time for the activation with NaOH and satisfactory consistencies for all the pastes.

Three poly(methacrylate-g-poly(ethylene glycol)) superplasticizers, supplied by CHRYSO SAINT-GOBAIN France, were used in this work. Their average structure can be described using Gay and Raphaël's nomenclature for comb copolymers [19,20]. The polymers are composed of *n* segments, each containing *N* backbone monomers and one side-chain of *P*

monomers. The superplasticizer average structures were *n8.5N5P17*, *n10N5P45* and *n10N5P114*. Thereafter, the polymers will be referred respectively as PCE17, PCE45, and PCE114 since only the side-chain length varied significantly. Their characteristic molecular parameters are given in Table 2. They were used as dilute solutions containing a defoamer and neutralized by NaOH. For the size-exclusion chromatography and the capillary viscometry measurements, solutions without defoamer were used. The water added by the polymer solution was considered in the calculation of the w/s ratio of the pastes. Except for the cloud point measurements, the superplasticizer used was PCE45, namely, the one with the medium length side-chains.

Table 2: Characteristic molecular parameters of the superplasticizers used.

Superplasticizer	n	N	P	M_w (g/mol)	M_n (g/mol)	Đ (M_w/M_n)
PCE17	8.5	5	17	31900	11000	2.9
PCE45	10	5	45	51000	25000	1.8
PCE114	10	5	114	152700	54500	2.8

2.2. Sample preparation and tests performed

A precise mass of polymer solution, depending on the dosage used and the dry extract of the solution, was firstly combined with the activating solution in a container with a diameter of 52 mm. Then, 50 g of slag was added into the solution. The alkali-activated slag paste was prepared by immediate mixing with an overhead stirrer, using a radial flow stirring blade of 29 mm diameter. The mixing procedure was the following. First, the paste was blended at 500 rpm for 30 s. Then, for an additional 30 s, a fast (1500 rpm) mixing was applied. This was followed by a rest time of 30 s and a final 1 min of fast mixing.

For adsorption and pore solution composition measurements, the slag pastes were left at rest for 10 min after the protocol described above and then homogenised by stirring for 1 min at 500

rpm. The resulting sample was filtered by two superimposed filter papers (20 - 25 µm and 11 µm particle retention) set in a Büchner funnel, using a vacuum pump. The aqueous phase was then filtered again with 1.2 µm PSE syringe membranes. This choice of a relatively coarse membrane insured that no polymer was retained by it when in good solvent and that the overall filtration process remained short enough (5 min) to neglect further advancement of hydration.

2.2.1. Isothermal micro-calorimetry

The hydration heat of the slag cements was measured at 25°C with a TAM Air isothermal micro-calorimeter from TA Instruments, at IETcc-CSIC (Madrid, Spain). A total mass of 5.0 g of cement paste was weighed into the mix-ampoules right after the mixing. The mix-ampoules were placed in the calorimeter at the same time as a reference composed of a precise mass of ultrapure water in order to have a similar calorific capacity as the cement samples. The resulting heat flows were normalised by the slag mass.

2.2.2. Polymer adsorption measurements

The amount of superplasticizer adsorbed on slag particles was determined by Total Organic Carbon (TOC) measurements using a TOC-L analyser from Shimadzu. For each activator, the TOC analyser was first calibrated with a "blank" sample (slag paste without any superplasticizer added) to assess the amount of organic carbon dissolved from the slag powder. The pore solutions, obtained as described above, were acidified with 20 % HCl to remove inorganic carbon and lower the pH to values tolerable by the analyser.

The affinity of the superplasticizers with the calcite surface was also assessed using the same protocol. Slag was replaced by calcite in quantities such as to keep the same total solid surface area.

2.2.3. Effect of the polymer on the slag paste rheology

The rheology of the samples was measured 5 min after the beginning of the mixing. Rheological parameters of pastes over time were determined at 25°C using a DHR 3 rheometer from TA Instruments equipped with a vane geometry. The paste rheological behaviour and the dispersing effect of the superplasticizers were characterized by determining flow curves. First, a shear ramp from 1 s^{-1} to 200 s^{-1} was applied for 1 min. This was followed by a 45 s pre-shearing at 200 s^{-1}. Finally, the flow curve was measured by steps of decreasing shearing rates from 200 s^{-1} to 0.01 s^{-1}. To ensure that the sample was in steady state conditions, points were taken only when the deviation of the torque stayed under 4.0 % during 3 s or if the measurement took more than 30 s to stabilize. This last case happened at very low shear rates, when the steady state could not be reached anymore, because the shearing energy was too low to fight the structuration of the pastes.

2.2.4. Polymer's chemical stability and size-exclusion chromatography (SEC)

The polymers were first diluted with the activating solutions for 30 min, at molalities of 3.2 mol/kg and 1.6 mol/kg for NaOH and Na_2CO_3 respectively. The solutions were then dialysed using a SpectraPor membrane (MWCO: 1 kDa) against ultrapure water. The water was changed every day until its pH reached the neutral value of 7. The polymers were then freeze-dried and subsequently redispersed in a 0.2 M $NaNO_3$ solution. The final solutions with a concentration in polymer of 2 g/L were analysed by SEC with a Viscotek TDA 302 system triple detector equipped with three OH-pak SB-806M HQ columns in series and a guard column. The mobile phase was a 0.2 M $NaNO_3$ aqueous solution and the flow-rate was 0.7 mL/min. 100 µL of each sample was passed in the set of columns. The number- and weight average molar masses (respectively M_n and M_w) and dispersity ($Đ=M_w/M_n$) were derived from a universal calibration curve based on poly(ethylene oxide) standards from Malvern.

2.2.5. Polymer cloud point measurements

The solubility of the polymers, depending on their side-chain length and the activator, was assessed by UV-visible spectroscopy and visual determination of their cloud point. The cloud point was defined in the following manner. Solutions of 1 g/L of polymer in ultrapure water were prepared. The activators were then added progressively until the solutions became turbid to the eye. The corresponding activator molality is called the cloud point. The validity of this qualitative cloud point procedure was checked by absorbance measurements with a UV–vis Hewlett-Packard 8453 spectrophotometer at a wavelength of 600 nm, using a quartz cell (see Supplementary material, Figure S1).

2.2.6. Polymer conformation and capillary viscometry

Changes in conformation of the superplasticizers in the activating solutions were estimated by capillary viscometry. Solutions containing different concentrations of polymer in the different activating solutions were prepared and studied with a Ubbelohde viscometer using a 0.53 mm diameter capillary tube. The apparatus' thermostat was set to 25°C. Each reported value is the average of 10 measurements.

The intrinsic viscosities [η] were obtained thanks to the empirical Fedors model [21] for polyelectrolyte solutions

$$\frac{1}{2\left(\sqrt{\eta_{sp}+1}-1\right)} = \frac{1}{[\eta]} \times \left(\frac{1}{C} - \frac{1}{C_m}\right) \qquad \text{Eq. 1}$$

where η_{sp} is the specific viscosity, C the polymer concentration and C_m the critical concentration corresponding to the particles close packing. This model was derived from an equation used for Newtonian suspensions of rigid particles and is generally suited for polymer solutions with specific viscosities comprised between 1 and 100.

Finally, the sizes of the superplasticizers were determined using the Fox-Flory [22,23] equation

$$[\eta] = \phi' \frac{R^3}{M} \qquad \text{Eq. 2}$$

that links the intrinsic viscosity to the polymers' radius *R* and to their molar mass *M*, and where ϕ' is equal to 3.08 x 10^{24} mol^{-1} for polymers with high polydispersities. It should be noted that the Fox and Flory theory was developed for dilute solutions of linear and flexible polymers in thermodynamic good solvent conditions. Consequently, the sizes calculated with this equation cannot be considered as true polymer sizes for the comb copolymers used, but it does provide the trend of the effect of the solvent on their size. We thus refer to the radius obtain from equation 2 as a viscosimetric radius.

2.2.7. Pore solution analysis by ICP-OES

Elementary composition of the pore solutions was measured at the ISTeP laboratory of Sorbonne Université (Paris, France) by Inductively Coupled Plasma – Optical Emission Spectrometry (ICP-OES) with a 5100 SVDV Agilent analyser. The interstitial solutions, obtained by filtration as explained above, were first acidified with HNO_3 2% in a proportion of 1:10 to prevent the precipitation of solids. The samples were then further diluted with HNO_3 2% to proportions of 1:1000, 1:200, 1:100 and 1:50 to explore different concentration ranges.

2.2.8. Characterization of the hydrates by X-Ray Diffraction (XRD)

To characterize the hydrates formed during the slag reaction with the different activators, the hydration of the samples was stopped after 9 h for the NaOH-activated pastes and after 131 h for the Na_2CO_3-activated. To stop them, the samples were washed twice with ultrapure water and then with isopropanol, following the protocol given by Palacios et al. [24]. Next, they were dried in a vacuum desiccator at room temperature and finely ground in a mortar. Finally, the powders obtained were analysed in a Phillips PW 1700 diffractometer equipped with a X'Celerator detector, in θ-2θ configuration. The X-rays corresponding to the Cupper $K_{\alpha 1}$ line (1.540562 Å) were produced with applied voltage and intensity of 40 kV and 40 mA respectively. Data were collected between 5 and 60°, with steps of 0.0170°.

2.2.9. Specific surface area measurements

The sample specific surface areas were obtained after krypton adsorption-desorption experiments at 77 K, using the BET method, by an external contractor (LIEC, Nancy, France). The measurements were conducted on an absorbometer Belsorp-Max II from MicrotracBEL Corp. The samples were degassed beforehand under vacuum to eliminate any superficial impurity. For calcite and anhydrous slag samples, the degassing was conducted at 120°C for 18 h. The specific surface area of cement pastes stopped right after the mixing was also assessed. These samples being more sensitive to thermal changes, the degassing was conducted at 80°C for 48 h.

3. RESULTS AND DISCUSSION

3.1. Hydration kinetics of the alkali-activated slag pastes

First and foremost, the kinetics of the hydration reaction of the activated and non-activated cements was studied by isothermal micro-calorimetry. The heat flows measured over 24 hours are presented on Figure 3. Only alkali-activated systems exhibited measurable heat flows due to the exothermic dissolution of the slag and hydrates precipitation. This indicates that (i) the hydration of slag in water was, as expected, very slow, and that (ii) the presence of activators was required for the cement to set.

Figure 3 also shows that the addition of superplasticizer to non-activated slag cements did not have any effect on its hydration. However, the superplasticizer had a small retarding effect on the hydration of the NaOH or Na_2CO_3 activated slags, since the heat flow peaks are delayed by 0.5 h and 3.5 h respectively.

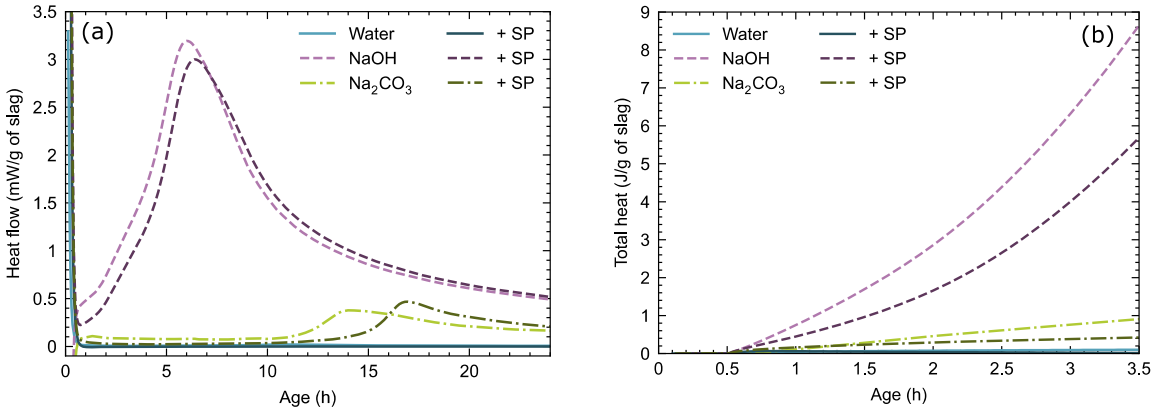

Figure 3: Isothermal micro-calorimetry measurements (25 °C) of the evolution of the heat flow over 24 hours (a) and of the total heat over 3.5 hours (b) of a slag cement hydrated in water (solid line), with Na_2CO_3- (dotted lines) or NaOH- (dashed lines) activations at 4%wt. Na_2O by weight of slag, and a w/s ratio of 0.4. Measurements were also performed in presence of 0.5 wt% (13.4 g/L) of the superplasticizer PCE45 (SP).

An important observation is that the heat released during the first fifteen minutes of hydration was minimal in all cases – not taking into account the initial dissolution heat. Even for the NaOH system, it remains at values typical of what is observed during ordinary cement dormant period (see for example results reported in [3]). Extrapolating to time zero the heat flux observed at 0.5 h, one can estimate an upper limit of 0.2 J/g slag for the heat released during the first 15 minutes in the most reactive (NaOH) system. Taking an approximate value of 300 J/g slag for the total heat of reaction[25], one infers that, at the very most, less than 1‰ of the slag had reacted after 15 minutes. Furthermore, Krypton adsorption measurements (Table 3) resulted in BET specific surface for samples stopped right after the mixing similar to the one of the initial anhydrous slag (see section 2.1.). This meant that even in the case of NaOH activation, the amount of surface area created during the first minutes of hydration could be neglected. In addition, XRD or NMR could detect no reaction products before a few hours (Figure S2). All these observations allow defining a 15 minutes-time window during which one can neglect hydrate formation, in first approximation. As a result, the following study of the superplasticizers was performed at hydration times within that time window, during which the

solid surface area can be considered constant and during which superplasticizer-hydrate interactions do not need to be considered on first analysis.

Table 3: Specific surface areas of non-activated, and 4%wt. Na_2O NaOH or Na_2CO_3-activated slag samples right after the mixing. The pastes were prepared with a w/s ratio of 0.4. The values are given with an error of ± 0.02 m^2/g.

System	Water	NaOH	Na_2CO_3
Kr BET (m^2/g)	0.82	0.85	0.83

3.2. Dispersing ability of the superplasticizer

The dispersing ability of the superplasticizer was assessed by flow curves measurements in the slag cements with different activator molalities. The samples were prepared at a constant w/s ratio of 0.4, but the activator quantity was varied between 4.0 and 0.5 wt% of Na_2O. Rheology experiments started five minutes after the beginning of the mixing and lasted about five minutes. Therefore, they took place before any important hydrates' precipitation, according to the calorimetry measurements (see Figure 3).

The results are presented in Figure 4 and show the expected rheological behaviours of cement pastes – which are yield stress fluids [26]. The yield stress τ_c is estimated by fitting the curves with the Herschel-Bulkley model:

$$\tau > \tau_c \Rightarrow \tau = \tau_c + k\dot{\gamma}^n \qquad \text{Eq. 3}$$

where τ is the shear stress, $\dot{\gamma}$ the strain rate, and k and n are material parameters. This empirical model is valid for steady state flow conditions with shear rates comprised between 10^{-2} and 100 s^{-1}. The behaviour of the slag pastes without any superplasticizer (Figures 4a and 4c) was similar whether the cement was activated or not, with a yield stress of 25 to 45 Pa. Moreover, the activator molality did not have a significant effect on the rheological behaviour of the slag pastes in these cases.

When the superplasticizer was added (Figures 4b and 4d), different behaviours appeared. In the case of a non-activated slag cement, i.e. in water, the addition of the superplasticizer led to a drastic decrease, below 1Pa, of the apparent yield stress. Even though the measurements were not done in steady state conditions anymore, this proves that the superplasticizer had a great dispersing ability in suspensions of slag in water.

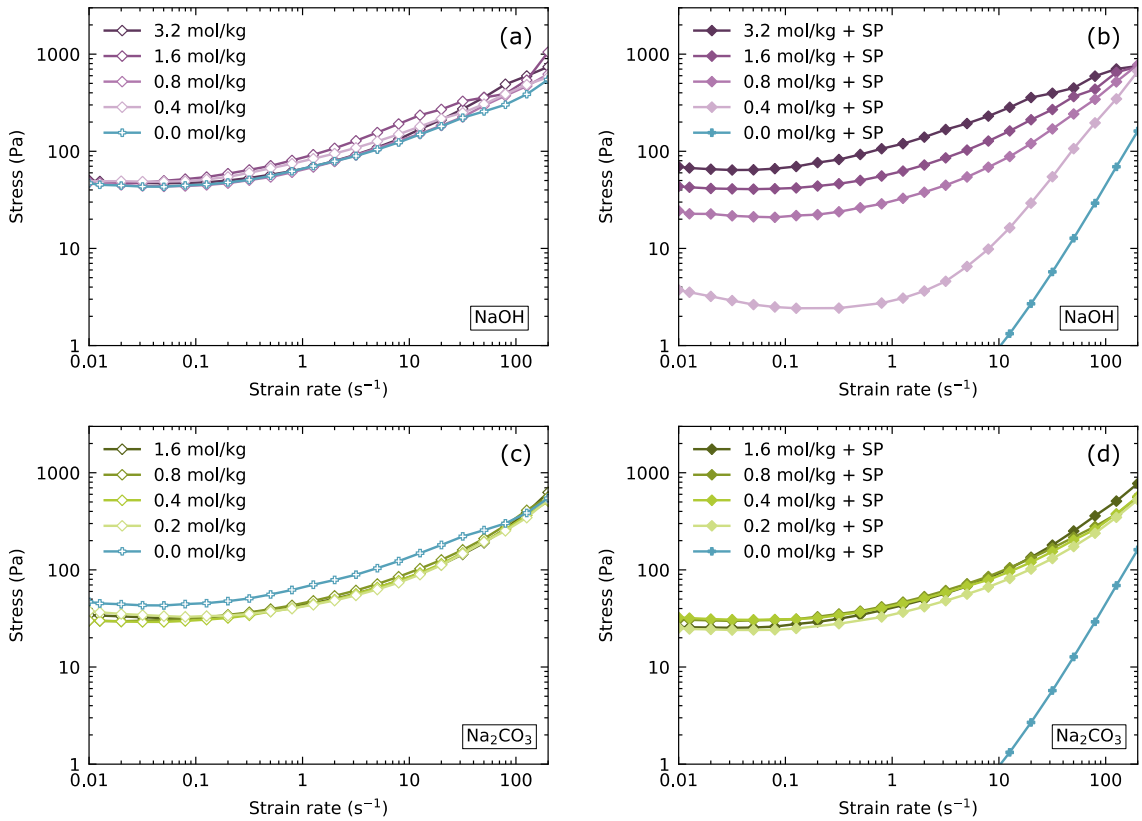

Figure 4: Flow curves obtained for slag cements activated with NaOH (a and b) and Na_2CO_3 (c and d), without (a and c) and with 0.5 wt% by slag (13.4 g/L) of PCE45 (b and d) depending on the activator molality. The w/s ratio is kept at 0.4, and the wt% of Na_2O is varied. For stresses under 1 Pa, systems are too fluid to be stable and sediment under gravitation forces. Results below 1 Pa are thus not reported.

On the contrary, the addition of the superplasticizer in alkali-activated slag pastes at 4.0 wt% of Na_2O and a w/s ratio of 0.4 (3.2 mol/kg of NaOH or 1.6 mol/kg of Na_2CO_3) was associated with negligible changes of rheological behaviour. For NaOH-activated slag (Figure 4b), some

297 fluidity was regained when the activator molality was diminished, but never reached the one
298 measured in non-activated slag cements. The Na_2CO_3 activation had an even worse effect on
299 the rheological curves, as it totally inhibited the dispersing effect of the superplasticizer at all
300 the concentrations investigated (Figure 4d).
301 In summary, the polymer could disperse slag particles in water, as expected, but lost this ability
302 in presence of activators, partially in the case of NaOH and totally in the case of Na_2CO_3. These
303 observations demonstrate that the efficiency problem of the superplasticizers was not due to an
304 intrinsic surface property of slag but to an effect of alkaline activators. Moreover, the two
305 activators did not have the same influence on the superplasticizer, as a gradual loss of efficiency
306 was observed with NaOH while Na_2CO_3 completely inhibited the polymer's action. Hence, the
307 two systems will be discussed separately for the remainder of the article.
308 First and foremost, the chemical stability of the PCEs in 3.2 mol/kg NaOH-solution or 1.6
309 mol/kg Na_2CO_3-solution was checked by SEC (Figure 5). It is established that the polymers
310 were not significantly hydrolysed in the activating solutions within the time scale of the
311 experiments as expected for superplasticizers with polymethacrylic acid backbones
312 (MPEG)[27]. Other hypothesis had to be explored to explain the PCEs efficiency losses in the
313 systems under investigations.

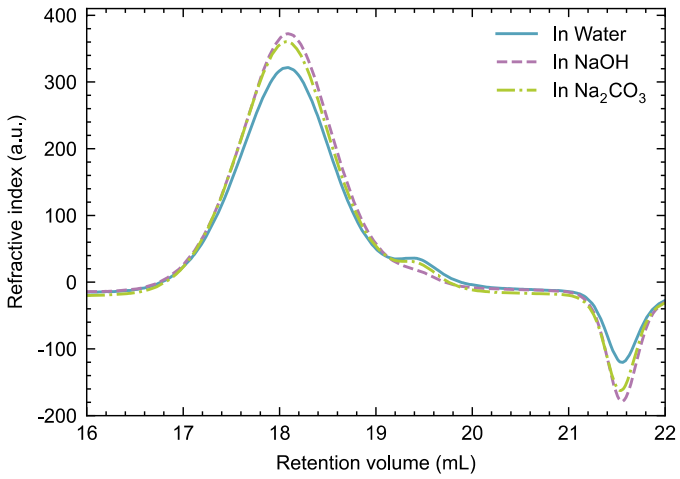

Figure 5: Size-exclusion chromatography curves showing the evolution of the refractive index depending on the retention volume for the superplasticizer PCE45 after contact with the activating solutions.

3.3. The case of NaOH-activation

3.3.1. Superplasticizer's adsorption on slag

As stated in the introduction, a possible explanation for the efficiency loss of the superplasticizer is a lack of adsorption of the polymer chains on slag grains. In order to explore this hypothesis, adsorption measurements were conducted on slag pastes with a higher w/s ratio of 0.8 to facilitate the collection of the interstitial solutions. The quantity of superplasticizer added to the system was varied to plot effective "adsorption isotherms" (Note that these measurements cannot be strictly considered as isotherms since they are not performed at thermodynamic equilibrium; furthermore, there is no guarantee that they solely reflect adsorption processes, as will be discussed below.). These analyses consisted in the measurement of the quantity of polymer in the interstitial solution of cement pastes with Total Organic Carbon equipment. Knowing the initial quantity of polymer added to the cement paste, the quantity of polymer removed from solution or adsorbed to the slag surface was then deduced. The results are presented on Figure 6a.

For both systems, the curves exhibit a generic Langmuir-type adsorption isotherm shape with a steep initial increase of the amount of adsorbed polymer, characteristic of a high polymer affinity for the surface of slag grains [9]. This increase is followed by an adsorption pseudo plateau corresponding to the full coverage of the slag particles' surface. The polymer's adsorption plateau in NaOH solutions or in pure water was reached for a similar value in both cases, around 0.8 mg/g corresponding to 0.95 mg/m^2.

These results indicate that the superplasticizer adsorption on slag was not modified in NaOH solutions, despite the loss of dispersing ability observed by rheology at the same NaOH

concentration (1.6 kg/mol). This result is different from the observations of Marchon et al. [17] who showed that the addition of NaOH in an OPC blended with fly ash leads to a decreased adsorption of PCEs. This difference was probably due to the contrast in composition and surface between clinker and slag particles. Indeed, the adsorption of the superplasticizers on slag was low compared to OPC systems (77 % of PCE remaining in solution at the plateau in our slag samples against 56 % in the OPC blended system [17]). Also, while the calcium concentration in solution is always relatively high and stable (imposed by portlandite equilibrium) in OPC systems, in slag it can vary. The use of NaOH activates slag hydration, making more calcium available to permit PCE adsorption (as seen in Table 5). This could counterbalance and mask a possible competitive adsorption of the hydroxides as observed in OPC.

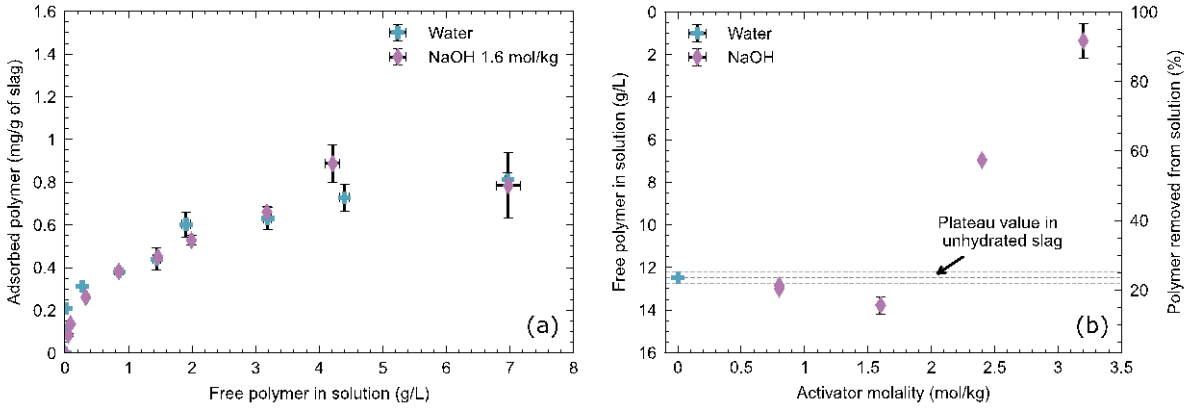

Figure 6: (a) Evolution of the quantity of adsorbed superplasticizer (PCE45) on non-activated or NaOH-activated slag depending on the quantity of free polymer in solution. The w/s ratio was 0.8, with 4.0 wt% of Na_2O by weight of slag when using NaOH, leading to a NaOH molality of 1.61 mol/kg. (b) Evolution of the quantity of free polymer (PCE45) (left axis) in solution or polymer removed from solution (right axis) depending on the NaOH molality. The superplasticizer was added in proportions of 0.6 wt% by weight of slag (16.9 g/L) and the w/s ratio was 0.4. The Na_2O dosage is varied to change the activator molality.

To further study the superplasticizer properties in the activated slag binders, adsorption measurements were conducted while varying the activators' molality. These experiments were

run on slag pastes with a w/s ratio of 0.4 and a polymer content of 0.6 wt% by weight of slag which is on the adsorption isotherm plateau. In order to change the activators' molality while keeping the initial quantity of polymer and the w/s ratio constant, the quantity of activator by weight of slag was varied from 0 wt%Na_2O to 4 wt% Na_2O for NaOH (maximum molality of 3.2 mol/kg).

The results are presented on Figure 6b. First, it can be noticed that, for a non-activated cement paste, i.e. in water, the quantity of free polymer in solution was 12.5 g/L, which corresponds to a little more than 20 % of the total polymer content adsorbed on slag surface under these conditions. For low NaOH molalities (0.8 and 1.6 mol/kg), polymer adsorption was similar to the one observed in non-activated conditions, as already seen in Figure 6a. For the highest NaOH concentrations in Figure 6b, the concentration of free polymer in solution decreased, leading to seemingly quasi total "adsorption" of polymer. This result was clearly not attributable to a Langmuir-type adsorption phenomenon. Another phenomenon than adsorption was at play here, which further separated the polymer from the interstitial solution.

3.3.2. Superplasticizer's solubility in NaOH solution

To investigate the phenomenon inducing a higher apparent adsorption of superplasticizers at high NaOH molality, the interaction between superplasticizers and activating solutions was studied independently from the slag. Indeed, during the paste preparations with a w/s ratio of 0.4 and 4.0 wt% of Na_2O, corresponding to an activator molality of 3.2 mol/kg for NaOH, it was observed that the addition of the superplasticizer to the activating solutions led to turbid solutions. However, this phenomenon did not occur when the superplasticizer was added in pure water. Hence, arises the question of the polymer solubility in the activating solutions.

The issue of superplasticizers solubility has been recently discussed by Conte and Plank [14] who showed by macroscopic observations that the solubility of PCEs can be insufficient in slag cements activated with NaOH or Na_2CO_3 and that this solubility depends on the side-chain length of the superplasticizers, their charge density and their chemical composition.

As in the study previously mentioned, the solubility of the superplasticizers was assessed by cloud point measurements at ambient temperature, and this for superplasticizers with different side-chain lengths (parameter *P* in Gay and Raphaël's nomenclature). The backbone chain length varied only slightly (parameter *n* from 8.5 to 10).

The cloud points were measured at polymer concentrations equal to the ones in [14] for sake of comparison. They are reported in Figure 7. The activator molalities corresponding to the cloud points were lower when the side-chain length was increased. This observation means that the polymer was more sensitive to the activator, and less soluble, for greater side-chain lengths.

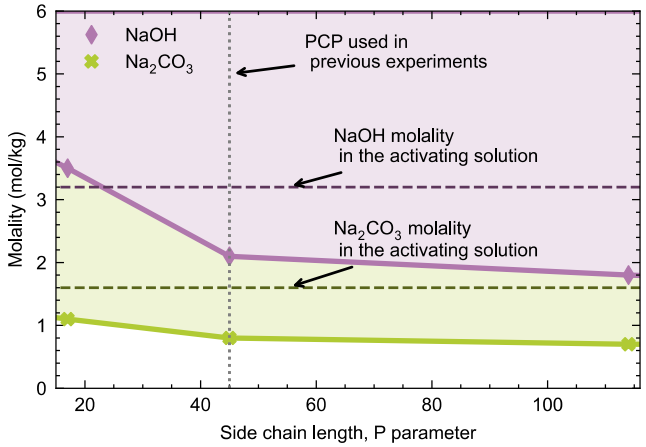

Figure 7: Cloud points measurements for superplasticizers with different side-chain lengths (*P*), at 1 g/L of polymer. For molality of activators higher than the cloud points, the polymer solutions were turbid.

It is now interesting to compare these results with the conditions used in the alkali-activated pastes. For slags activated with 4.0 wt% of Na_2O by weight of slag and a w/s ratio of 0.4, the NaOH molality is 3.2 mol/kg. As figured by the corresponding horizontal dashed line in Figure

7, this molality did not correspond to a swollen state for PCE45 and PCE114, meaning these polymers were not fully soluble even at the low polymer concentration of 1 g/L. They are likely to be even less soluble at the higher concentrations of 13-17 g/L used in the present study. Only the superplasticizer with small side-chains, PCE17, was in a swollen state at this NaOH molality.

The absence of dispersing effect of the superplasticizer (Figure 4b) and the aberrant values of adsorption (Figure 6b) in activated cements at 3.2 mol/kg of NaOH can thus be explained by a first order phase transition from dispersed to aggregated states. Indeed, this concentration being above the cloud point of PCE45, the decrease of solubility of the polymers led to their aggregation. The polymer was then retained by the filters used for the collection of the interstitial solution, inducing very high apparent "adsorptions" (Figure 6b). Furthermore, the PEG side-chains are collapsed and not extended in the interstitial solution under these conditions and cannot play their role of steric repulsion between the slag's particles (Figure 4b), potentially accounting for the loss of efficiency of the superplasticizer.

However, a transition from solvated to aggregated states cannot explain the observed loss of efficiency below the cloud point. A better solubility of the polymers can be obtained either by lowering the activator molality (going from the top to the bottom of Figure 7) or by reducing the side chain length (going from the left to the right of Figure 7). Some rheology measurements were thus conducted with PCE17 in non-activated and NaOH-activated slag (w/s of 0.4, 4.0 wt% of Na_2O, 3.2 mol/kg of NaOH), as shown on Figure S3 in the Supplementary Material. This superplasticizer did improve the fluidity of the non-activated slag but lost its efficiency in the NaOH-activated paste, even though its "cloud point" is above the NaOH molality in these conditions. This result is similar to what was observed with PCE45. Indeed, Figure 4b showed that PCE45 had no dispersing ability in NaOH-activated slag at a molality of 1.6 mol/kg, which is also slightly below the PCE45 "cloud point" in NaOH solution. Furthermore, as seen in

Figure 4b, the fluidity of PCE45 did not transition abruptly when going above the cloud point. Instead, the loss was gradual when the NaOH molality increased toward the cloud point, a behaviour that is not compatible with a first order phase transition from solvated to aggregated state. Solubility in its strict sense cannot fully account for the fluidity loss.

3.3.3. Influence of NaOH on the superplasticizer's viscometric radius

To further investigate potential conformational changes of the superplasticizers in the NaOH solution below its cloud point, the PCE45 solutions specific viscosities were measured by capillary viscometry. Variations of specific viscosities reveal conformational changes and allow to estimate qualitatively variations of the hydrodynamic size of the superplasticizer according to Fedors model[20,21]. Since this model is strictly valid only for polymers in their swollen state, the measurements were done in water and in NaOH at 1.61 mol/kg, which corresponds to the molality used previously for the adsorption isotherm (Figure 6a). Furthermore, it was verified that all solutions (polymer concentrations from 0 to 14 g/L) were clear (below their cloud points) and the polymers could be considered as swollen.

The evolution of the specific viscosities depending on the polymer concentration is plotted on Figure 8 and the values are fitted with Fedors model (Eq. 1). The intrinsic viscosities and the viscometric radii obtained from the Fox-Flory equation are reported in Table 4. A significant decrease of the superplasticizer viscosimetric radii was observed in the NaOH-solution compared to the pure water solution, even though the NaOH molality used were below the cloud point and thus corresponded to swollen state conditions.

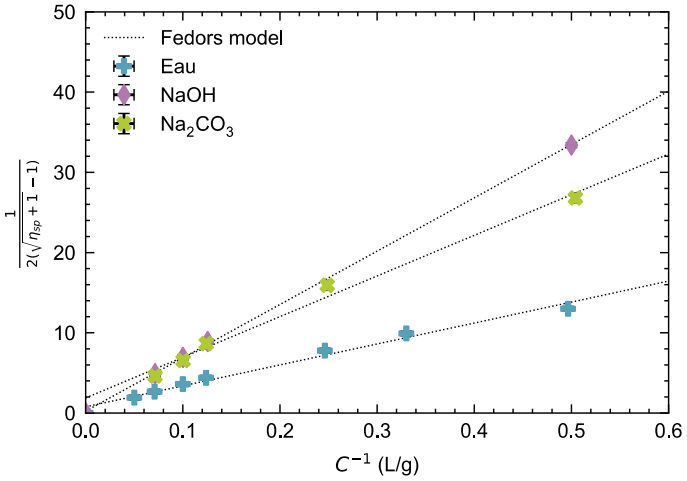

Figure 8: Evolution of the polymer (PCE45) solutions' specific viscosity depending on the polymer concentration from 0 to 14 g/L. The values are plotted accordingly to Fedors model in order to obtain the intrinsic viscosity of the superplasticizer in the different solutions. The activator molalities were 1.61 mol/kg for the NaOH solution and 0.65 mol/kg for the Na_2CO_3 solution. All solutions were clear and thus below their cloud points.

Table 4: Intrinsic viscosities and viscometric radii of the superplasticizer in water, 1.61 mol/kg of NaOH, or 0.65 mol/kg of Na_2CO_3, calculated with the Fedors equation and the Fox and Flory model (see part 2.2.5.). The values are given with an error of ± 2 mL/g for the intrinsic viscosities and ± 0.2 nm for the viscometric radii.

	Water	**NaOH**	**Na_2CO_3**
Intrinsic viscosity (mL/g)	39	15	20
Viscometric radius (nm)	8.6	6.3	6.8

To further study this effect, the activator molality was decreased, keeping the polymer concentration constant (2 g/L). The specific viscosities measured are presented in Figure 9, without using Fedors model as the polymer concentration was kept constant. The specific viscosities decreased only slowly with the activator molality but eventually reached the value measured in pure water for a molality of 0.002 mol/kg. Therefore, the polymer radius increased when the NaOH molality decreased. Interestingly, the viscosities were always lower than the

one of PCE in pure water despite the fact that all these measurements were performed in clear solutions (not turbid).

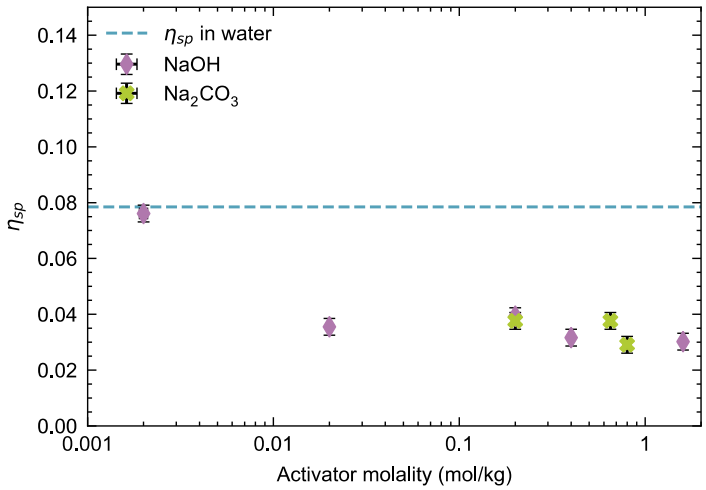

Figure 9: Evolution of the polymer (PCE45) solutions' specific viscosity depending on the activator molality. The polymer concentration was 2 g/L.

These experiments showed that, even when the polymer solutions were macroscopically clear, the presence of NaOH led to a decrease of the solvent quality for the superplasticizers and thus to its partial shrinking, as represented on Figure 10. The side-chains were not extended in the solution and could not play their role of steric repulsion between the slag grains. As NaOH molality decreases, the solvent quality improved and the side-chains further expanded in the interstitial solution. The dispersing action was hence gradually recovered.

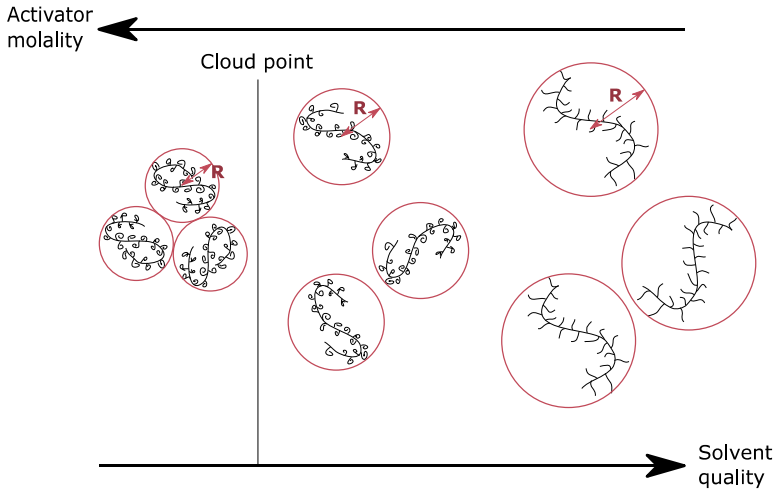

Figure 10: Schematic representation of the evolution of the polymer's conformation depending on the solvent quality. R is the polymer's viscometric radius.

It can thus be concluded that the lack of efficiency of the superplasticizers in NaOH-activated slag cements is not simply due to a phase separation when they are not in a swollen state but also to a gradual decrease of the solvent quality with the concentration of the NaOH activating solution, which limits the steric repulsion of the side-chains. The question now is to see if the same explanation for the efficiency loss of PCE applies to Na_2CO_3 activation or if other phenomena must be explored.

3.4. The case of Na_2CO_3-activation

3.4.1. Superplasticizer adsorption on slag

First, as for NaOH, the adsorption behaviour of the superplasticizer PCE45 was studied in Na_2CO_3-activated systems. This time, two w/s ratios (0.8 and 1.0) were used to see the effect of the Na_2CO_3 molality on the effective adsorption isotherms. The curves obtained (Figure 11) present a different shape than the previous isotherms obtained with NaOH (Figure 6a): the initial slope was slower compared to non-activated and NaOH-activated slag no apparent inflexion point marked the approach to a plateau value. For PCE45 concentrations below 2.5 g/L, effective adsorption appeared generally reduced in the Na_2CO_3 system compared to non-activated and NaOH-activated slag. This meant that contrary to NaOH, the Na_2CO_3 solution significantly disturbs the polymer adsorption. This result does not depend on the w/s ratio (nor on the activator molality) indicating that mainly surface adsorption phenomena are at play at low concentrations of polymer. For PCE45 concentrations above 2.5 g/L, on the other hand, and for a w/s ratio of 0.8, corresponding to the highest Na_2CO_3 concentration, no plateau is observed and the amount reached is even higher than the one resulting from adsorption observed in water. This last result is confirmed by the results shown in Figure 11b where increasing

adsorption values and less polymer in the interstitial solution are observed as the Na_2CO_3 molality is increased up to 6 wt% Na_2O for Na_2CO_3 (maximum molalities of 2.4 mol/kg). These results reflect that as for NaOH, at high concentration of polymers, a phenomenon other than simple physical adsorption is at play.

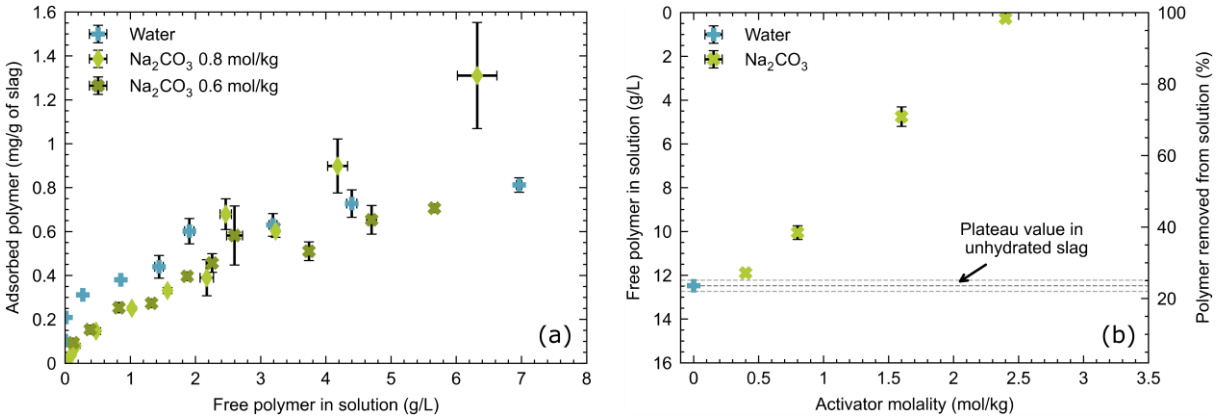

Figure 11: (a) Evolution of the quantity of adsorbed superplasticizer on slag without an activator (in water) or activated with Na_2CO_3 depending on the quantity of free polymer in solution. The non-activated paste had a w/s ratio of 0.8. The Na_2CO_3 samples were all activated with 4.0 wt% Na_2O by weight of slag, and two w/s ratio were tested: 0.8 corresponding to a Na_2CO_3 molality of 0.81 mol/kg, and 1.0 corresponding to a molality of 0.65 mol/kg. (b) Evolution of the quantity of free polymer (PCE45) (left axis) in solution or polymer removed from solution (right axis) depending on the Na_2CO_3 molality. The superplasticizer was added in proportions of 0.6 wt% by weight of slag (16.9 g/L) and the w/s ratio was 0.4. The Na_2O dosage is varied to change the activator molality.

3.4.2. Superplasticizer solubility in Na_2CO_3 solution

As well as for the NaOH system, the high adsorption values observed can be explained by a lack of solubility of the superplasticizers in the Na_2CO_3 solutions. Indeed, the cloud points measurements conducted (see Figure 7) showed that the addition of Na_2CO_3 also impacted the solvent quality for the superplasticizers, leading to even lower values of cloud points with Na_2CO_3 than with NaOH. This trend, which follows the Hofmeister series, is common when

studying the solubility of PEG [28–30], or of polymers containing PEG segments[31], and is linked to the higher valency and radius of CO_3^{2-} compared to OH^- [32]. Furthermore, as for NaOH, the capillary viscometry measurements resulted in a lower viscometric radius of PCE45 in 0.65 mol/kg Na_2CO solutions than in pure water (Figure 8, Table 4 and Figure 9).

However, the dispersing ability of the superplasticizers was not gradually recovered when using lower molalities of Na_2CO_3 (Figure 4d), contrary to the NaOH-activated system. This shows that the lack of solubility and the change of conformation were not the only phenomena at play here. The mechanisms were thus more complex and warranted further investigations.

3.4.3. Investigation of the lower superplasticizer adsorption in Na_2CO_3 systems

As was shown in section 3.4.1., the adsorption of the superplasticizer on the slag particles was modified when the cement was activated with Na_2CO_3. Two possible explanations are examined hereafter.

The first conjecture is that the calcium concentration in the interstitial solution was too low. Indeed, it is well known that calcium cations serve as a link between the negatively charged surface of cementitious or slag particles and the negative backbone of the superplasticizers. However, even though the calcium concentration in solutions (Table 5) was lower in Na_2CO_3-activated pastes (as well as in NaOH-activated pastes) compared to what is measured in ordinary Portland cement [33,34], the value was similar to the one obtained for non-activated slag cement. The previous observations thus cannot be explained by a lower calcium concentration in the interstitial solution.

Table 5: Calcium concentrations in the interstitial solution of the different slag cements, measured by ICP-OES. The values are given with an error of ± 6 µmol/L.

System	Water	NaOH	Na_2CO_3
[Ca] mmol/L	0.406	0.750	0.437

The second conjecture is a preferential adsorption of the superplasticizer on reaction products which would have already been formed in low quantities even at early hydration times. The activated slags were thus analysed by XRD at different times of reaction. The results are presented on Figure 12. The anhydrous slag leads to a diffractogram with a large bump around 30° corresponding to its amorphous content. Some small peaks were also visible which can be associated with the presence of a low quantity of vaterite in the initial slag.

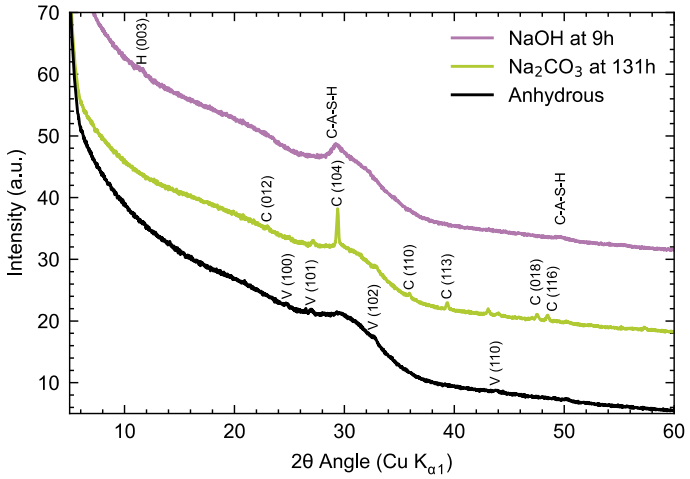

Figure 12: X-ray diffractograms of anhydrous slag and of the NaOH- and Na_2CO_3-activated slag cements, with a w/s ratio of 0.4 and 4.0 wt% of Na_2O. The peaks are referenced with the corresponding Miller indexes between brackets according to the PDF files. The different phases visible are $CaCO_3$ crystallised as calcite (noted C, file 00-005-0586) and as vaterite (noted V, file 01-072-0506), hydrotalcite $Mg_2Al(OH)_4(CO_3)_{0.5}H_2O$ (noted H, file 01-089-0460) and a C-A-S-H taken accordingly to the tobermorite-11Å structure (file 00-045-1480).

When slag was activated with NaOH, peaks corresponding to a C-A-S-H gel [35–38] was present at 9 h, as it is the primary hydration product of cementitious binders, together with some peaks corresponding to hydrotalcite as a secondary hydrate. In the case of an activation with Na_2CO_3, calcite [36,39] was detected at 131 h, as well as a very amorphous alumino-silicate gel, mostly visible on the NMR spectra (Figure S2).

As a result, adsorption measurements of the superplasticizer on calcite were conducted to investigate if the formation of this phase could explain the apparent lower adsorption values measured previously in the case of Na_2CO_3 activation (Figure 11). Indeed, one could conjecture that due to high concentration of carbonates some very small calcite crystallites, undetectable by XRD, would be already formed at the time of the adsorption measurements and that the superplasticizer would adsorb on them. The TOC apparatus would still measure this fraction of the PCE as part of the solution since some calcite crystallites could be small enough to pass through the 1.2 µm filters used to separate the interstitial solution. Different studies [40–44] have already shown that superplasticizers can adsorb well on calcite and that this mineral can be used as a reference system for early-age cementitious materials. This is a plausible hypothesis that is explored in the following paragraph.

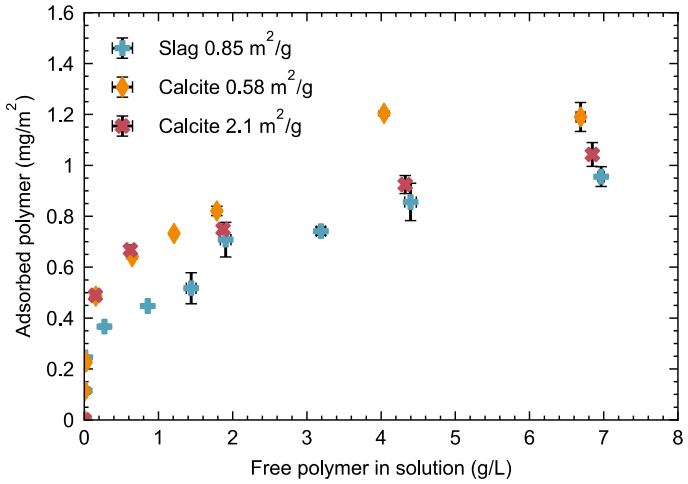

Figure 13: Adsorption isotherms of the superplasticizer PCE45 on slag and two calcites of different specific surface area. These experiments were conducted with a constant total surface of solid corresponding to the samples at w/s = 0.8.

The adsorption isotherms on slag and calcite are presented on Figure 13. Contrary to what was done for the previous adsorption studies, in this case, it is better to look at the values given in mg/m^2 of solid since they take into account the different specific surface areas of calcite and

slag. For this purpose, we have considered that the specific surface area of the slag was not significantly changed during the first 15 minutes of reaction (see Table 3).

Figure 12 shows that the quantities of superplasticizer adsorbed on calcite are equal or a little higher than on slag. Therefore, the polymer could indeed adsorb on the calcite precipitated in the Na_2CO_3-activated slag pastes. Nevertheless, taking the Ca concentration measured by ICP-OES in the liquid phase of this sample (0.4 mmol/L, see Table 5) as an estimate of the order of magnitude of Ca precipitated as calcite nuclei, the quantity of polymer adsorbed on calcite at the plateau (1.1 mg/m^2) cannot account for the difference of adsorbed polymer between the Na_2CO_3- or non-activated samples (5.5 mg/m^2 according to the data of Figure 11). The specific surface of the calcite crystallites needed for this hypothesis to be true can be estimated to 3500 m^2/g. This very high value is aberrant as it would require crystallite sizes of the atomic order. The orders of magnitude involved are thus not in favour of the calcite adsorption hypothesis.

Consequently, the competitive adsorption of the polymers on calcite cannot by itself explain the lower affinity of the superplasticizers to the slag surface in Na_2CO_3-activated systems. However, the formation of calcite showed there is a strong interaction between Ca^{2+} and CO_3^{2-}. Therefore, there could be a competition between the CO_3^{2-} anions and the superplasticizers for the adsorption sites at the slag surface, explaining the shape of the isotherms measured previously (Figure 11). This last explanation, however plausible, could not be tested with the experimental means of the current study and thus remains hypothetical.

4. CONCLUSIONS

This paper provides results on the behaviour of polycarboxylates ether superplasticizers in alkali-activated slag. Two systems were considered, with NaOH and Na_2CO_3 as alkaline activators.

First and foremost, it was shown that the dispersing efficiency of the superplasticizers in non-activated slag cement was good, with satisfying adsorption and rheological behaviours. The

chemical stability of the polymers in the activating solutions was also confirmed by SEC analyses. Therefore, the question of the solubility of the superplasticizers in the activating solutions (NaOH and Na_2CO_3), which has only been investigated once before, was examined. A qualitative correlation between the solubility of the polymers and the adsorption measures was found. However, the full dispersing ability of the polymers, as manifested in the rheology of the paste, was not retrieved in the swollen state. Capillary viscometry was thus conducted to study the conformation of the polymers in the corresponding activating solutions. A smaller viscometric radius was measured for the superplasticizers in the NaOH and Na_2CO_3 solutions. Since the viscometric radius of comb copolymers scales with the coil size of the side-chains, this meant that the side-chain extension was also reduced. This could very well lead to a degradation of the steric repulsion between particles, which is the mechanism of action of superplasticizers, thus explaining their loss of efficiency in alkali-activated slag cements.

Furthermore, it appeared that the superplasticizer adsorption as well was hindered in Na_2CO_3-activated slag cements. This observation could not be explained by the low Ca concentration in the cement pore solution nor by the competitive adsorption of the superplasticizer between the slag and the precipitated calcite. Finally, by elimination, the most plausible hypothesis seemed to be a competitive adsorption between the superplasticizer and the CO_3^{2-} brought by the activator but this remained an open question.

To summarize, it was found that the solubility of MPEG polymers in NaOH and Na_2CO_3 activating solutions represents a limiting factor for their dispersing capability. Furthermore, the presence of activator anions alters both the adsorption of the polymer and its conformation. The present study thus suggests that, to improve the rheology of alkali-activated slag cements, it will be necessary to formulate polymers less sensitive to the ionic strength of the activating solutions than the superplasticizers currently used by the industry in ordinary Portland cements.

CRediT authorship contribution statement

Clara Paillard: Conceptualisation, Methodology, Investigation, Writing – Original Draft, Visualization; **Marien Aparicio Cordoba**: Investigation; **Nicolas Sanson**: Conceptualization, Methodology, Writing – Review & Editing, Supervision; **Jean-Baptiste d'Espinose de Lacaillerie**: Conceptualization, Methodology, Writing – Review & Editing, Supervision; **Guylaine Ducouret**: Methodology; **Pascal Boustingorry**: Conceptualisation, Methodology, Writing – Review & Editing; **Marie Jachiet**: Conceptualization, Methodology, Writing – Review & Editing; **Claire Giraudeau**: Conceptualisation, Methodology, Writing – Review & Editing; **Vanessa Kocaba**: Conceptualization, Methodology, Writing – Review & Editing.

Declaration of competing interests

The authors declare that there is no conflict of interest.

ACKNOWLEDGEMENT

This research was solely funded by CHRYSO SAINT-GOBAIN and by the SIMM laboratory supervisory authorities (CNRS, ESPCI Paris PSL and Sorbonne Université). It did not receive any specific grant from funding agencies in the public, commercial, or not-for-profit sectors. The authors gratefully acknowledged extremely helpful discussions concerning calorimetry and rheology protocols with Dr. Marta Palacios and Dr. Nicolas Roussel.

REFERENCES

[1] F.G. Collins, J.G. Sanjayan, Workability and mechanical properties of alkali activated slag concrete, Cement and Concrete Research. 29 (1999) 455–458. https://doi.org/10.1016/S0008-8846(98)00236-1.

[2] A. Fernández-Jiménez, F. Puertas, Effect of activator mix on the hydration and strength behaviour of alkali-activated slag cements, Advances in Cement Research. 15 (2003) 129–136. https://doi.org/10.1680/adcr.2003.15.3.129.

[3] A. Gruskovnjak, B. Lothenbach, L. Holzer, R. Figi, F. Winnefeld, Hydration of alkali-activated slag: comparison with ordinary Portland cement, Advances in Cement Research. 18 (2006) 119–128. https://doi.org/10.1680/adcr.2006.18.3.119.

[4] J.S.J. Van Deventer, J.L. Provis, P. Duxson, Technical and commercial progress in the adoption of geopolymer cement, Minerals Engineering. 29 (2012) 89–104. https://doi.org/10.1016/j.mineng.2011.09.009.

[5] T. Tsubakimoto, M. Hosoido, H. Tahara, Copolymer and method for manufacture thereof, US4471100A, 1984.

[6] P.F.G. Banfill, A discussion of the papers “rheological properties of cement mixes” by M. Daimon and D. M. Roy, Cement and Concrete Research. 9 (1979) 795–796. https://doi.org/10.1016/0008-8846(79)90075-9.

[7] E.M. Gartner, H. Koyata, P. Scheiner, Influence of aqueous phase composition on the zeta potential of cement in the presence of water-reducing admixtures, American Ceramic Society. 40 (1994) 131–140.

[8] G. Gelardi, R.J. Flatt, 11 - Working mechanisms of water reducers and superplasticizers, in: P.-C. Aïtcin, R.J. Flatt (Eds.), Science and Technology of Concrete Admixtures, Woodhead Publishing, 2016: pp. 257–278. https://doi.org/10.1016/B978-0-08-100693-1.00011-4.

[9] D. Marchon, S. Mantellato, A.B. Eberhardt, R.J. Flatt, 10 - Adsorption of chemical admixtures, in: P.-C. Aïtcin, R.J. Flatt (Eds.), Science and Technology of Concrete Admixtures, Woodhead Publishing, 2016: pp. 219–256. https://doi.org/10.1016/B978-0-08-100693-1.00010-2.

[10] E. Douglas, J. Brandstetr, A preliminary study on the alkali activation of ground granulated blast-furnace slag, Cement and Concrete Research. 20 (1990) 746–756. https://doi.org/10.1016/0008-8846(90)90008-L.

[11] F. Puertas, A. Palomo, A. Fernández-Jiménez, J.D. Izquierdo, M.L. Granizo, Effect of superplasticisers on the behaviour and properties of alkaline cements, Advances in Cement Research. 15 (2003) 23–28.

[12] M. Palacios, F. Puertas, Effect of superplasticizer and shrinkage-reducing admixtures on alkali-activated slag pastes and mortars, Cement and Concrete Research. 35 (2005) 1358–1367. https://doi.org/10.1016/j.cemconres.2004.10.014.

[13] M. Palacios, F. Puertas, Stability of superplasticizer and shrinkage-reducing admixtures in high basic media, Materiales de Construcción. 54 (2004) 65–86.

[14] T. Conte, J. Plank, Impact of molecular structure and composition of polycarboxylate comb polymers on the flow properties of alkali-activated slag, Cement and Concrete Research. 116 (2019) 95–101. https://doi.org/10.1016/j.cemconres.2018.11.014.

678 [15] A. Habbaba, J. Plank, Interaction between polycarboxylate superplasticizers and
679 amorphous ground granulated blast furnace slag, Journal of the American Ceramic
680 Society. 93 (2010) 2857–2863. https://doi.org/10.1111/j.1551-2916.2010.03755.x.
681 [16] A. Habbaba, J. Plank, Surface chemistry of ground granulated blast furnace slag in
682 cement pore solution and its impact on the effectiveness of polycarboxylate
683 superplasticizers, Journal of the American Ceramic Society. 95 (2012) 768–775.
684 https://doi.org/10.1111/j.1551-2916.2011.04968.x.
685 [17] D. Marchon, U. Sulser, A. Eberhardt, R.J. Flatt, Molecular design of comb-shaped
686 polycarboxylate dispersants for environmentally friendly concrete, Soft Matter. 9 (2013)
687 10719–10728. https://doi.org/10.1039/C3SM51030A.
688 [18] J. Plank, C. Hirsch, Impact of zeta potential of early cement hydration phases on
689 superplasticizer adsorption, Cement and Concrete Research. 37 (2007) 537–542.
690 https://doi.org/10.1016/j.cemconres.2007.01.007.
691 [19] C. Gay, E. Raphaël, Comb-like polymers inside nanoscale pores, Advances in Colloid
692 and Interface Science. 94 (2001) 229–236. https://doi.org/10.1016/S0001-
693 8686(01)00062-8.
694 [20] G. Gelardi, N. Sanson, G. Nagy, R.J. Flatt, Characterization of Comb-Shaped
695 Copolymers by Multidetection SEC, DLS and SANS, Polymers. 9 (2017) 61.
696 https://doi.org/10.3390/polym9020061.
697 [21] R.F. Fedors, An equation suitable for describing the viscosity of dilute to moderately
698 concentrated polymer solutions, Polymer. 20 (1979) 225–228.
699 https://doi.org/10.1016/0032-3861(79)90226-X.
700 [22] M. Rubinstein, R.H. Colby, Polymer physics, Oxford University Press, Oxford ; New
701 York, 2003.
702 [23] P.J. Flory, Principles of Polymer Chemistry, Cornell University Press, 1953.
703 [24] M. Palacios, S. Gismera, M.M. Alonso, J.B. d'Espinose de Lacaillerie, B. Lothenbach,
704 A. Favier, C. Brumaud, F. Puertas, Early reactivity of sodium silicate-activated slag
705 pastes and its impact on rheological properties, Cement and Concrete Research. 140
706 (2021) 106302. https://doi.org/10.1016/j.cemconres.2020.106302.
707 [25] M. Königsberger, J. Carette, Validated hydration model for slag-blended cement based
708 on calorimetry measurements, Cement and Concrete Research. 128 (2020) 105950.
709 https://doi.org/10.1016/j.cemconres.2019.105950.
710 [26] N. Roussel, Understanding the rheology of concrete, Woodhead Publ., Oxford, 2012.
711 [27] G. Gelardi, S. Mantellato, D. Marchon, M. Palacios, A.B. Eberhardt, R.J. Flatt, 9 -
712 Chemistry of chemical admixtures, in: P.-C. Aïtcin, R.J. Flatt (Eds.), Science and
713 Technology of Concrete Admixtures, Woodhead Publishing, 2016: pp. 149–218.
714 https://doi.org/10.1016/B978-0-08-100693-1.00009-6.
715 [28] F.E. Bailey, R.W. Callard, Some properties of poly(ethylene oxide)1 in aqueous
716 solution, Journal of Applied Polymer Science. 1 (1959) 56–62.
717 https://doi.org/10.1002/app.1959.070010110.
718 [29] H.D. Willauer, J.G. Huddleston, R.D. Rogers, Solute Partitioning in Aqueous Biphasic
719 Systems Composed of Polyethylene Glycol and Salt: The Partitioning of Small Neutral
720 Organic Species, Industrial & Engineering Chemistry Research. 41 (2002) 1892–1904.
721 https://doi.org/10.1021/ie010598z.

[30] M.J. Hey, D.P. Jackson, H. Yan, The salting-out effect and phase separation in aqueous solutions of electrolytes and poly(ethylene glycol), Polymer. 46 (2005) 2567–2572. https://doi.org/10.1016/j.polymer.2005.02.019.

[31] B.A. Deyerle, Y. Zhang, Effects of Hofmeister Anions on the Aggregation Behavior of PEO–PPO–PEO Triblock Copolymers, Langmuir. 27 (2011) 9203–9210. https://doi.org/10.1021/la201463g.

[32] Y. Marcus, ViscosityB-coefficients, structural entropies and heat capacities, and the effects of ions on the structure of water, Journal of Solution Chemistry. 23 (1994) 831–848. https://doi.org/10.1007/BF00972677.

[33] F. Caruso, S. Mantellato, M. Palacios, R.J. Flatt, ICP-OES method for the characterization of cement pore solutions and their modification by polycarboxylate-based superplasticizers, Cement and Concrete Research. 91 (2017) 52–60. https://doi.org/10.1016/j.cemconres.2016.10.007.

[34] D. Rothstein, J.J. Thomas, B.J. Christensen, H.M. Jennings, Solubility behavior of Ca-, S-, Al-, and Si-bearing solid phases in Portland cement pore solutions as a function of hydration time, Cement and Concrete Research. 32 (2002) 1663–1671. https://doi.org/10.1016/S0008-8846(02)00855-4.

[35] A. Fernández-Jiménez, F. Puertas, Setting of alkali-activated slag cement. Influence of activator nature, Advances in Cement Research. (2001) 7.

[36] A. Fernández-Jiménez, F. Puertas, I. Sobrados, J. Sanz, Structure of calcium silicate hydrates formed in alkaline-activated slag: influence of the type of alkaline activator, Journal of the American Ceramic Society. 86 (2003) 1389–1394. https://doi.org/10.1111/j.1151-2916.2003.tb03481.x.

[37] R.J. Myers, S.A. Bernal, J.L. Provis, Phase diagrams for alkali-activated slag binders, Cement and Concrete Research. 95 (2017) 30–38. https://doi.org/10.1016/j.cemconres.2017.02.006.

[38] F. Bonk, J. Schneider, M.A. Cincotto, H. Panepucci, Characterization by multinuclear high-resolution nmr of hydration products in activated blast-furnace slag pastes, Journal of the American Ceramic Society. 86 (2003) 1712–1719. https://doi.org/10.1111/j.1151-2916.2003.tb03545.x.

[39] A.R. Sakulich, S. Miller, M.W. Barsoum, Chemical and microstructural characterization of 20-month-old alkali-activated slag cements, Journal of the American Ceramic Society. 93 (2010) 1741–1748. https://doi.org/10.1111/j.1551-2916.2010.03611.x.

[40] G. Bossis, P. Boustingorry, Y. Grasselli, A. Meunier, R. Morini, A. Zubarev, O. Volkova, Discontinuous shear thickening in the presence of polymers adsorbed on the surface of calcium carbonate particles, Rheologica Acta. 56 (2017) 415–430. https://doi.org/10.1007/s00397-017-1005-4.

[41] F. Dalas, A. Nonat, S. Pourchet, M. Mosquet, D. Rinaldi, S. Sabio, Tailoring the anionic function and the side chains of comb-like superplasticizers to improve their adsorption, Cement and Concrete Research. 67 (2015) 21–30. https://doi.org/10.1016/j.cemconres.2014.07.024.

[42] N. Mikanovic, K. Khayat, M. Pagé, C. Jolicoeur, Aqueous CaCO3 dispersions as reference systems for early-age cementitious materials, Colloids and Surfaces A: Physicochemical and Engineering Aspects. 291 (2006) 202–211. https://doi.org/10.1016/j.colsurfa.2006.06.042.

[43] S. Pourchet, S. Liautaud, D. Rinaldi, I. Pochard, Effect of the repartition of the PEG side chains on the adsorption and dispersion behaviors of PCP in presence of sulfate, Cement and Concrete Research. 42 (2012) 431–439. https://doi.org/10.1016/j.cemconres.2011.11.011.

[44] J.A. Richards, R.E. O'Neill, W.C.K. Poon, Turning a yield-stress calcite suspension into a shear-thickening one by tuning inter-particle friction, Rheologica Acta. 60 (2021) 97–106. https://doi.org/10.1007/s00397-020-01247-z.